Journal of Power Sources 263 (2014) 154–157

Contents lists available at ScienceDirect

Journal of Power Sources

journal homepage: www.elsevier.com/locate/jpowsour

Short communication

Highly effective Pt/$MoSi_2$ composite counter electrode catalyst for dye-sensitized solar cell

Mingxing Wu [a,*], Ya-nan Lin [a], Hongyue Guo [a], Tingli Ma [b], Anders Hagfeldt [c]

[a] College of Chemistry and Material Science, Key Laboratory of Inorganic Nano-materials of Hebei Province, Hebei Normal University, No. 20 Rd. East of 2nd Ring South, Yuhua District, Shijiazhuang City, Hebei Province 050024, PR China
[b] Department State Key Laboratory of Fine Chemicals, School of Chemistry, Dalian University of Technology, No. 2 Linggong Road, Ganjingzi District, Dalian City, Liaoning Province 116024, PR China
[c] Department of Physical and Analytical Chemistry, Uppsala University, Box 259, SE–751 05 Uppsala, Sweden

HIGHLIGHTS

- $MoSi_2$ is proposed as CE catalysts for DSC for the first time.
- Highly effective Pt/$MoSi_2$ composite catalysts have been prepared.
- The DSC using Pt/$MoSi_2$ composite CE yield a high PCE value of 7.68%.

ARTICLE INFO

Article history:
Received 30 January 2014
Accepted 7 April 2014
Available online 18 April 2014

Keywords:
$MoSi_2$
Catalyst
Composite
Counter electrode
Solar cell
Pt

ABSTRACT

$MoSi_2$ is introduced into dye-sensitized solar cell (DSC) as counter electrode (CE) catalyst for the first time, and the DSC produces power conversion efficiency (PCE) of 4.87%. To improve the catalytic activity, Pt/$MoSi_2$ composite catalyst is synthesized and it is found that 1.13 wt% of Pt loading is enough for achieving high catalytic activity. After optimization, the DSC using the Pt/$MoSi_2$ composite CE shows high PCE of 7.68%, close to the Pt CE based DSC (7.94%).

1. Introduction

Dye-sensitized solar cell (DSC), as a third-generation solar cell, is a promising candidate to the silicon solar cells because of the strengths of simple assembly procedure, good plasticity, environmental friendliness, and ease of building combination. In recent years, DSC is undergoing a revival, accompanying with great advancement in each component of DSC, comprising semiconductor, dye, electrolyte and counter electrode (CE) catalysts [1,2]. However, as the cost reduction of the commercial silicon solar cell, to realize long term developments and practical application of DSC still requires robust decrease of the production cost. Fortunately, develop low-cost counter electrode (CE) catalysts is one of promising paths to reduce the production cost to replace the expensive Pt CE. A class of Pt-free catalysts have been used as CE catalysts, such as carbon materials [3,4], organic polymers [5,6], and metal compounds [7–10].

Amongst these metal compounds, the carbides draw great attentions due to the typical Pt-like behavior [11]. Recently, we used commercial and synthesized molybdenum carbide (C–Mo_2C and S–Mo_2C) as CE catalysts in DSC [12,13]. The C–Mo_2C and S–Mo_2C based DSC showed PCE value of 5.70% and 5.83%, indicating that Mo_2C indeed present the Pt-like catalytic behavior in DSC system. As with the carbide, silicide also belongs to the interstitial compound, the properties of which have been changed significantly originating from the exotic atom (Si) intrusion, as compared to the body metal (Mo). Thus the silicide have been used in several fields of heating elements, structural parts at elevated temperature, and lithium-ion batteries due to the advantages of high melting point, high electrical conductivity, and good oxidation resistance at high temperature [14–16]. To the authors' knowledge, silicide is rarely applied in

*Corresponding author. Tel./fax: +86 311 80787438.
E-mail addresses: mingxing@mail.ustc.edu.cn, mingxingwu_paper@163.com (M. Wu).

http://dx.doi.org/10.1016/j.jpowsour.2014.04.029
0378-7753/

catalysis, especially work as the CE catalyst in DSC. Herein, we fabricated DSC by using molybdenum silicide ($MoSi_2$) and Pt/$MoSi_2$ composite CE for the first time, which were expected to be worked as effective as the carbide. In addition, the morphology, electrochemical process, and the impact of Pt loading on the catalytic activity have also been investigated with the techniques of SEM, EIS, CV, etc.

2. Experimental

2.1. Synthesis of $MoSi_2$/Pt

100 mg of $MoSi_2$ powder was dispersed in 5 mL isopropanol under stirring, followed by adding 100, 200, 300, or 400 μL of chloroplatinic acid isopropanol solution (containing 1 g of chloroplatinic acid and 100 mL of isopropanol). The solution was then dispersed under stirring for 30 min and then transferred to a dry oven to remove the isopropanol and got the precursor of $MoSi_2$ absorbed with chloroplatinic acid. Finally, sinter the $MoSi_2$/chloroplatinic acid at 480 °C for 30 min under N_2 atmosphere, collected the Pt/$MoSi_2$ composites with different Pt contents of 0.38, 0.76, 1.13 and 1.50 wt%, denoted as Pt/$MoSi_2$-1, Pt/$MoSi_2$-2, Pt/$MoSi_2$-3, and Pt/$MoSi_2$-4.

2.2. Cell fabrication

$MoSi_2$ and Pt/$MoSi_2$ CE were prepared as follow: 100 mg of $MoSi_2$ (or Pt/$MoSi_2$) was dispersed in 4 mL of isopropanol. The solution was then ultrasonically dispersed for 30 min to achieve the spray paste. The prepared paste was then coated onto FTO glass with an air brush (spray gun). Subsequently, the FTO glass coated with $MoSi_2$ (or Pt/$MoSi_2$) film was sintered under N_2 atmosphere at 350 °C for 30 min and the CE were prepared. The DSC was fabricated with a photoanode, a CE, and an electrolyte. The active area of the DSC was 0.16 cm^2. Symmetrical cell was fabricated with two identical CE clipping the electrolyte. The cells were sealed with a hot-melt surlyn film. The photoanode used in this work was an 8 μm thick TiO_2 film sensitized with N719 dye. The electrolyte contains 0.1 M of LiI, 0.6 M 1-propyl-3-methylimidazolium iodide, 0.07 M I_2, 0.5 M 4-tert-butyl pyridine, and 0.1 M guanidinium thiocyanate in 3-methoxypropionitrile (MPN).

2.3. Measurements

X-ray diffraction (XRD) measurements were carried out with an automatic X-ray powder diffractometer (D/Max 2400, Rigaku). The morphologies of $MoSi_2$ and Pt/$MoSi_2$ were characterized by scanning electron microscopy (SEM, S-4800, Hitachi, Japan). Electrochemical impedance spectroscopy (EIS) and Tafel-polarization, and cyclic voltammetry (CV) experiments were characterized with an electrochemical workstation system (CHI 660E, Chenhua Shanghai). In EIS, the measured frequency ranged from 100 m Hz to 1 M Hz. The amplitude of the alternating current was set at 10 mV. In CV measurements, Pt served as the CE and Ag/Ag^+ worked as the reference electrode. The I^-/I_3^- electrolyte contained 0.1 M $LiClO_4$, 10 mM LiI, and 1 mM I_2 in acetonitrile. The current photovoltaic performance of the DSC was carried out under simulated AM 1.5 illumination (I = 100 mW cm^{-2}, PEC-L01, Peccell, Yokohama, Japan) with the electrochemical workstation CHI 660E.

3. Results and discussion

3.1. Characterization of the prepared $MoSi_2$ and Pt/$MoSi_2$ CE

Although $MoSi_2$ powder can be synthesized via so many routes [17–19], we use the commercial $MoSi_2$ with high purity to prepare CE in this work due to the fact that impurities impact the catalytic activity strikingly. Fig. 1(a) presents the XRD patterns of $MoSi_2$ before and after loading with Pt. The diffraction peaks at 22.54, 29.94, 39.52, 44.45, 45.97, 57.13, 62.20, 65.83, 71.79, 75.13, 76.28, 85.19 can be assigned to the crystal planes of (002), (101), (110), (103), (112), (200), (202), (211) (006), (213), (204), and (116) for $MoSi_2$ (PDF-2 database, no. 81-0164). In the case of $MoSi_2$/Pt, we can only observe the strongest diffraction peak at 39.74°, assigned to the crystal planes of (111) for Pt (PDF2-database, no. 04-0802) due to poor crystallinity.

SEM images in Fig. 1(b) and (c) show the top morphology of the $MoSi_2$ and Pt/$MoSi_2$. The $MoSi_2$ particle size was uneven, from 500 nm to 5 μm. Before loading Pt, the surface of $MoSi_2$ particle was smooth, while clear white points on the surface can be observed on the $MoSi_2$ particle surface after loading Pt, and the white points referred to the deposited Pt particle. Fig. 1(d) was the energy-dispersive X-ray spectroscopy (EDS) image and the inset was the close-up EDS profile, indicating the existence of a certain amount of Pt. These XRD and EDS results prove that Pt/$MoSi_2$ composite has been synthesized successfully.

3.2. Photovoltaic performance of the DSC using the prepared $MoSi_2$ and Pt/$MoSi_2$ as CEs

First, $MoSi_2$ was applied as CE in DSC, which produced a PCE of 4.87%, much lower the Pt CE based DSC (7.94%), and the fill factor (FF) was only 0.52, implying an unsatisfactory catalytic activity. The photocurrent–density voltage (J–V) curve and the photovoltaic parameters are listed in Fig. 2(a) and Table 1, respectively. To improve the catalytic activity, we attempted to deposit Pt particle on $MoSi_2$ surface to synthesize composite catalyst. In this work, we prepared four Pt/$MoSi_2$ composites containing different Pt loading of 0.38, 0.76, 1.13 and 1.50 wt%, denoted as Pt/$MoSi_2$-1, Pt/$MoSi_2$-2, Pt/$MoSi_2$-3, and Pt/$MoSi_2$-4, respectively. Then, these Pt/$MoSi_2$ composites were used as CEs in DSC. Fig. 2(b) shows the J–V curve of the DSC using Pt/$MoSi_2$composite CEs. In the case of Pt/$MoSi_2$-1, the DSC exhibited a PCE of 6.79%, an obvious enhancement in PCE compared to the pristine $MoSi_2$, originating from 0.38 wt% of Pt loading. In details, as compared to the pristine $MoSi_2$, adding a little Pt loading of 0.38 wt% can increase the short-circuit density (J_{sc}) from 12.84 to 14.91 mA cm^{-2}; FF increase from 0.52 to 0.63. While there were no visible change for the open-circuit voltage (V_{oc}). Adding more Pt to $MoSi_2$ can further increase the catalytic activity. As the Pt loading increased to 1.13%, the DSC gave the optimal PCE of 7.68%, and the FF increased to 0.68 (J_{sc} = 15.71, FF = 0.68, V_{oc} = 719 mV). However, continuous increase of Pt loading did not enhance the catalytic activity obviously. That is to say, adding 1.13 wt% Pt into $MoSi_2$ is enough to obtain higher catalytic activity. The superiorities of the Pt/$MoSi_2$ based DSC were the growing J_{sc} and FF values, caused by the constantly enhanced catalytic activity of the Pt/$MoSi_2$ composite CE. Thus, loading a little amount of Pt is an effective method to obtain a highly effective catalyst. The composite CE could greatly reduce the quantity of Pt consumption, subsequently reducing the cost of DSC without sacrificing the PCE value.

3.3. Electrocatalytic process of the prepared Pt, $MoSi_2$, and Pt/$MoSi_2$ electrodes in iodide electrolyte

As adding 1.13 wt% of Pt loading is enough to obtain the best catalytic activity, in the following section we used the Pt/$MoSi_2$-3 CE to carry out a series of experiments. CV was applied to reveal the catalytic process of the Pt/$MoSi_2$ electrode in the iodide electrolyte. Fig. 3 gives the typical voltammograms. For Pt, two typical pairs of redox peaks were observed which can be assigned to two redox

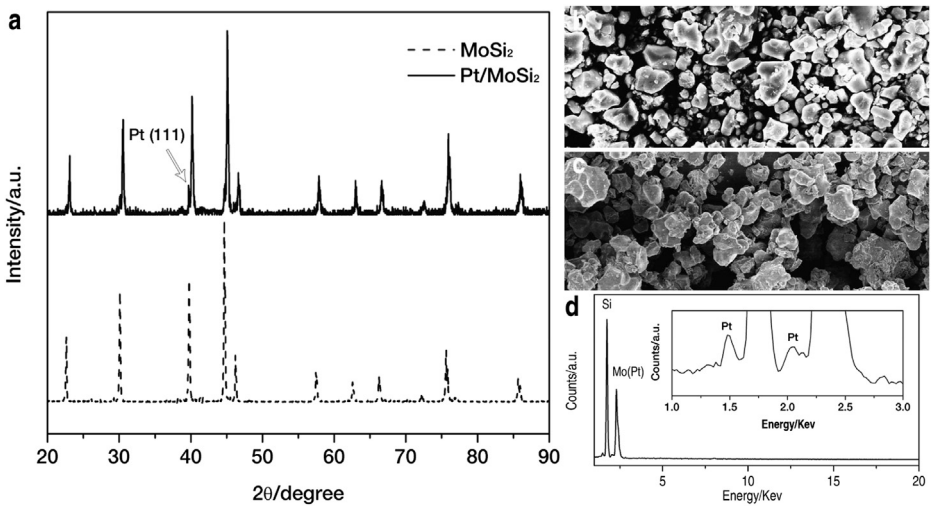

Fig. 1. (a) XRD patterns of $MoSi_2$ and $Pt/MoSi_2$; SEM images of (b) $MoSi_2$ and (c) $Pt/MoSi_2$; (d) EDS of $Pt/MoSi_2$, the inset is the close-up EDS profile.

reactions [20]. However, for $MoSi_2$, the oxidation peak at high potential was indistinct. In addition, the current density of $MoSi_2$ was much lower than Pt. The CV result proved that $MoSi_2$ cannot work as effectively as Pt for iodide redox couples regeneration. When adding Pt to $MoSi_2$, two pairs of redox peaks appeared, and the voltammogram showed a perfect appearance. Besides, the current density was evidently enhanced for $Pt/MoSi_2$ compared with pristine $MoSi_2$. For the primary redox peaks (left pair), the cathodic peak of $Pt/MoSi_2$ moved toward positive, whereas the anodic peak moved toward negative. In other words, the ΔE_p (peak-to-peak separation) for $Pt/MoSi_2$ was narrower than $MoSi_2$. Theoretically, ΔE_p varies inversely with the charge transfer rate (k_s) [12,21]. Thus we can deduce that the k_s value of $Pt/MoSi_2$ was much higher than $MoSi_2$. Moreover, the low ΔE_p indicated that $Pt/MoSi_2$ had a better reversibility than $MoSi_2$. The CV results indicated the smoothness of the redox reaction of the triiodide/iodide on the $Pt/MoSi_2$ electrode, which produced favorable conditions for the regeneration of the sensitizer. This finding confirms that Pt loading is a feasible method to produce an economical but effective catalyst.

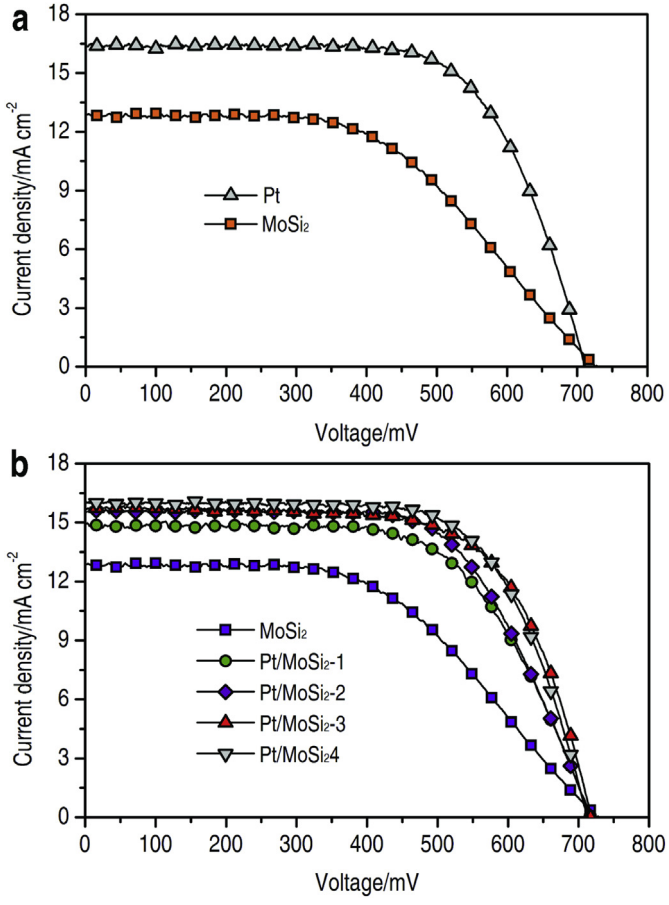

Fig. 2. (a) Current density–voltage (J–V) curves of the DSC using Pt and $MoSi_2$ CEs; (b) J–V curves of the DSC using $Pt/MoSi_2$ CEs contain different Pt loading.

EIS experiments were performed with symmetrical cells fabricated with two identical electrodes to investigate the electrochemical process for $Pt/MoSi_2$, which related closely with the catalytic activity. Fig. 4(a) shows the EIS spectra of the typical Nyquist plots. The high frequency intercept on the real axis corresponds to the series resistance (R_s). The left arch at the high-frequency region can be assigned to the charge transfer resistance (R_{ct}) at the electrode/electrolyte interface, which dominates the catalytic activity to a certain extent; the other arch at the low-frequency region arises from the Nernst diffusion impedance (Z_N) of the triiodide/iodide. The values of the EIS parameters were obtained by fitting the EIS plots with an equivalent circuit (inset in Fig. 4(a)). The R_s values for Pt, $MoSi_2$, and $Pt/MoSi_2$ could be considered the same. The R_{ct} value of Pt was 1.7 Ω cm^2, while the R_{ct} value of $MoSi_2$ (8.1 Ω cm^2) was several times higher than Pt, indicating $MoSi_2$ owned a lower catalytic activity as compared with Pt. In contrast, when deposited Pt on $MoSi_2$, the R_{ct} value was reduced to 1.9 Ω cm^2, implying an enhanced catalytic activity, close to Pt. EIS results verified that $Pt/MoSi_2$ behaved more effectively than $MoSi_2$

Table 1
Photovoltaic parameters of the DSC using different CEs.

Counter electrodes	V_{oc}/mV	J_{sc}/mA cm^{-2}	FF	PCE/%
Pt	712	16.39	0.68	7.94
$MoSi_2$	729	12.84	0.52	4.87
$Pt/MoSi_2$-1	718	14.91	0.63	6.94
$Pt/MoSi_2$-2	719	15.58	0.65	7.28
$Pt/MoSi_2$-3	719	15.71	0.68	7.68
$Pt/MoSi_2$-4	714	16.01	0.68	7.77

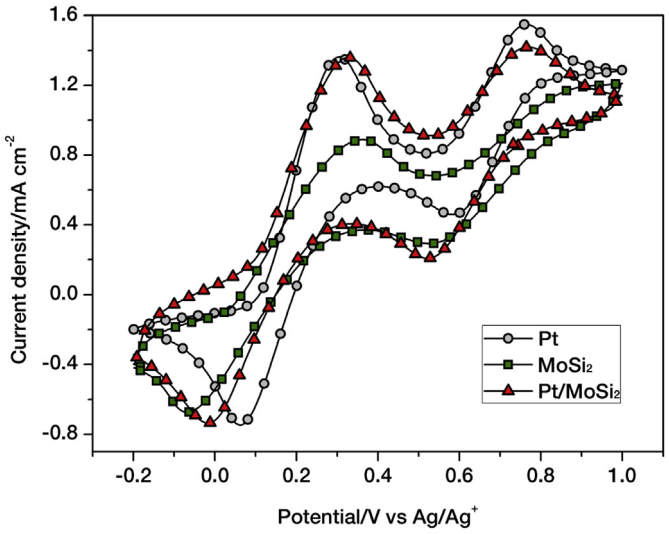

Fig. 3. Cyclic voltammograms of the Pt, $MoSi_2$, and Pt/$MoSi_2$ electrodes for iodide electrolyte.

for triiodide reduction and that Pt loading was a promising path to obtain high catalytic activity.

In attention to EIS test, Tafel curves were also performed. As showed in Fig. 4b, the curves depicted logarithmic current density (J) as a function of voltage (U) and a detailed analysis of the Tafel polarization can be obtained in our previous work [12]. The exchange current density (J_0) of $MoSi_2$ was much lower than that of Pt, implying that $MoSi_2$ had a lower catalytic activity than Pt. Whereas the curve of Pt/$MoSi_2$ exhibited a higher J_0 compared with $MoSi_2$, indicating that Pt/$MoSi_2$ performed much better than $MoSi_2$. In theory, J_0 varies inversely with R_{ct} [22]. The change tendency of J_0, deduced from the EIS results, is generally in accordance with those presented in the Tafel curves. After a comprehensive analysis of the CV, EIS, and Tafel polarization results, it is evident that the catalytic activity can be enhanced by deposit Pt on $MoSi_2$ to form a composite catalysis and this method can reduce the Pt consumption simultaneously.

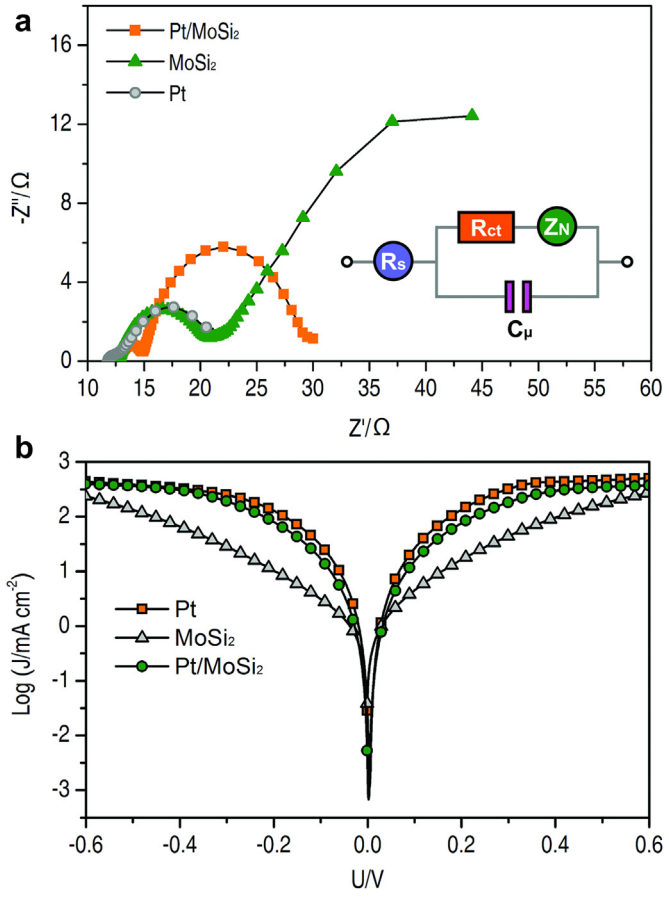

Fig. 4. (a) Nyquist plots and (b) Tafel polarization curves of the symmetrical cells using Pt, $MoSi_2$, and Pt/$MoSi_2$ electrodes. Inset in (a) is the equivalent circuit diagram.

4. Conclusions

In summary, silicide was successfully applied as CE catalyst in DSC system. Moreover, to enhance the catalytic activity $MoSi_2$/Pt composite catalysts were prepared by an in situ chemical method which can reduce the Pt consumption without compromising catalytic activity. The impact of Pt loading on the catalytic activity was investigated and found that 1.13 wt% Pt loading was enough to achieve an outstanding activity. The author though that design economical composite CEs is an effective method for reducing the cost of DSC.

Acknowledgements

This research was supported by the National Natural Science Foundation of China (Grant No. 21303039), Natural Science Foundation of Hebei Province (Grant No. B2013205171), Support Program for Hundred Excellent Innovation Talents from the Universities of Hebei Province, BR2–220), and Scientific Research Foundation for Introduction of Talents of Hebei Normal University.

References

[1] B.E. Hardin, H.J. Snaith, M.D. McGehee, Nat. Photonics 6 (2012) 162–169.
[2] A. Yella, H.-W. Lee, H.N. Tsao1, C. Yi, A.K. Chandiran, M.K. Nazeeruddin, E.W.-G. Dia, C.-Y. Yeh, S.M. Zakeeruddin, M. Grätzel, Science 334 (2011) 629–634.
[3] X. Xu, D. Huang, K. Cao, M. Wang, S.M. Zakeeruddin, M. Grätzel, Sci. Rep. 3 (2013) 1489.
[4] C. Bu, Y. Liu, Z. Yu, S. You, N. Huang, L. Liang, X.-Z. Zhao, ACS Appl. Mater. Interfaces 5 (2013) 7432–7438.
[5] X. Yan, L. Zhang, J. Appl. Electrochem. 43 (2013) 605–610.
[6] Y. Qiu, S. Lu, S. Wang, X. Zhang, S. He, T. He, J. Power Sources 253 (2013) 300–304.
[7] J.S. Jang, D.J. Ham, E. Ramasamy, J. Lee, J.S. Lee, Chem. Commun. 46 (2010) 8600–8602.
[8] A.-R. Ko, J.-K. Oh, Y.-W. Lee, S.-B. Han, K.-W. Park, Mater. Lett. 65 (2011) 2220–2223.
[9] J. He, N.W. Duffy, J.M. Pringle, Y.-B. Cheng, Electrochim. Acta 105 (2013) 275–281.
[10] M. Wu, L. Mu, Y. Wang, Y. Lin, H. Guo, T. Ma, J. Mater. Chem. A 1 (2013) 7519–7524.
[11] R.B. Levy, M. Boudart, Science 181 (1973) 547–549.
[12] M. Wu, X. Lin, Y. Wang, L. Wang, W. Guo, D. Qi, X. Peng, A. Hagfeldt, M. Grätzel, T. Ma, J. Am. Chem. Soc. 134 (2012) 3419–3428.
[13] M. Wu, X. Lin, A. Hagfeldt, T. Ma, Angew. Chem. Int. Ed. 50 (2011) 3520–3524.
[14] W. Li, X. Zhang, C. Hong, W. Han, J. Han, Scr. Mater. 60 (2009) 100–103.
[15] J. Xu, H. Wu, B. Li, Int. J. Refract. Met. Hard Mater. 28 (2010) 217–220.
[16] F.M. Courtel, D. Duguay, Y. Abu-Lebdeh, I.J. Davidson, J. Power Sources 202 (2012) 269–275.
[17] T. Yamada, H. Yamane, J. Alloys Compd. 509 (2011) L23–L25.
[18] S. Hasani, M. Panjepour, M. Shamanian, J. Therm. Anal. Calorim. 107 (2012) 1073–1081.
[19] J.V. Rau, R. Teghil, D. Ferro, A. Generosi, V.R. Albertini, M. Spoliti, S.M. Barinov, Thin Solid Films 518 (2010) 2050–2055.
[20] M. Wu, X. Lin, T. Wang, J. Qiu, T. Ma, Energy Environ. Sci. 4 (2011) 2308–2315.
[21] R.S. Nicholson, Anal. Chem. 37 (1965) 1351–1355.
[22] M. Wu, Y. Wang, X. Lin, W. Guo, K. Zhong, Y. Lin, H. Guo, T. Ma, J. Mater. Chem. A 1 (2013) 9672–9679.